

Electronic Supplementary Information

Magnetic Ionic Liquids Based On Transition-metal Complexes with N-Alkylimidazole Ligands

Deepak Chand,^a Muhammad Qamar Farooq,^a Arjun K. Pathak^b Jingzhe Li^a Emily A. Smith^a and
Jared L. Anderson^{*a}

*^aDepartment of Chemistry, Iowa State University, 1605 Gilman Hall, Ames,
IA 50011, USA. E-mail: andersoj@iastate.edu; Tel: +1 515-294-8356.*

*^bDivision of Materials Science and Engineering, Ames Laboratory, Iowa State
University, 254 Spedding, Ames, IA 50011, USA.*

Table of Contents

1. Viscosity Measurement
2. Raman Spectroscopy
3. Infrared Spectroscopy
4. Experimental Section
5. Thermal Properties (DSC and TG)
6. Magnetic Properties (SQUID magnetic measurements)
7. References

Viscosity measurements

A Brookfield Ametek DV1MRV digital viscometer (viscosity range 100-13, 300,000 cP) equipped with a CPA-51Z spindle was used to measure the viscosity of MILs. A MIL volume of 0.5 mL was used, and the measurements were performed at 21.7 °C using a speed of 20 rpm for a time period of 60 s.

Raman spectroscopy

Raman spectroscopy measurements were performed on bulk ionic liquids samples using a XploRA Plus confocal Raman microscope (HORIBA Scientific, Edison, NJ) equipped with a 20× (0.40 NA) long working distance objective. A 785-nm laser operating at 0.8 mW ($\sim 2\text{W}/\text{cm}^2$) was used for excitation and the average of 5 areas with 3 accumulation of 30s acquisition was acquired for each sample. The data were plotted using IGOR (WaveMetrics, Portland, OR).

The Raman peaks of the MILs are generally a superimposition of the corresponding 1-alkylimidazole and LiNTf_2 spectra, however, the changes derived from the specific interaction in the MILs are notable. The experimental peak position was obtained by fitting the measured peaks to a Gaussian profile as well as using a multi-fitting program when peaks were not well resolved. The Raman peaks assignments of the imidazole ring vibrations are based on previous reports.¹⁻³ The blue shift of several imidazole ring vibrations for the MIL peaks compared to 1-alkylimidazole peaks reflects an interaction between the metal and imidazole that is consistent with the FT-IR data.

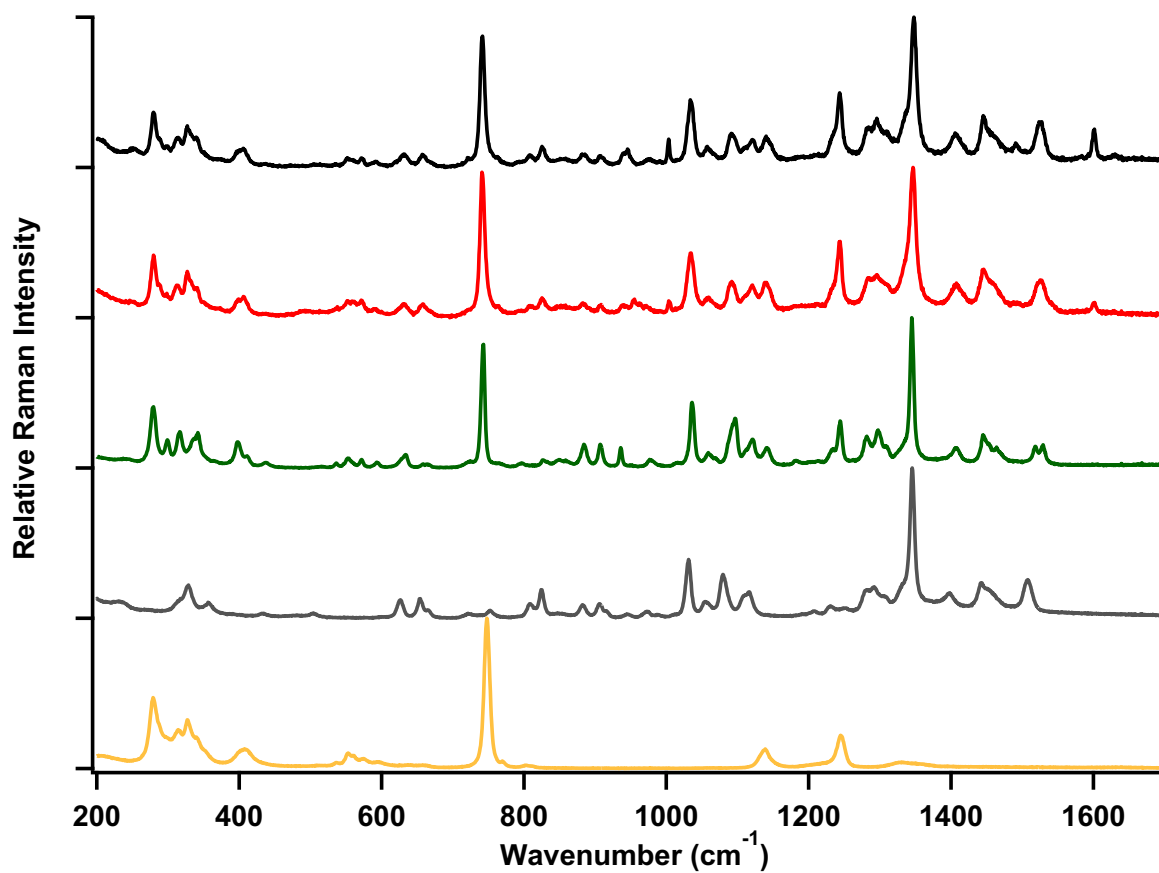


Figure S1. Normalized Raman spectra of Ni(BIm)₄(Cl)NTf₂ (black), Co(BIm)₄(Cl)NTf₂ (red), Mn(BIm)₄(Cl)NTf₂ (green), 1-butylimidazole (grey) and LiNTf₂ (yellow).

Table S1. Imidazole ring vibrations, in cm^{-1} , of $\text{Ni}(\text{BIm})_4(\text{Cl})\text{NTf}_2$, $\text{Co}(\text{BIm})_4(\text{Cl})\text{NTf}_2$, $\text{Mn}(\text{BIm})_4(\text{Cl})\text{NTf}_2$ and 1-butyylimidazole as measured and assignment of these vibrations from the literature.

$\text{Ni}(\text{BIm})_4(\text{Cl})\text{NTf}_2$	$\text{Co}(\text{BIm})_4(\text{Cl})\text{NTf}_2$	$\text{Mn}(\text{BIm})_4(\text{Cl})\text{NTf}_2$	1- Butylimidazole	Imidazolium- containing ILs ¹⁻³	Assignment ¹⁻³
631	631	632	626	600	b (ring op), v $\text{CH}_2(\text{N})$ CN
658	657	657	654	622-624	b (ring op), v $\text{CH}_2(\text{N})$ CN
669	668	667	665	655	b (ring op)
1034	1034	1036	1031	1022-1025	v (ring sym ip)
1347	1346	1345	1345	1339-1340	v (ring sym ip, $\text{CH}_2(\text{N})$ CN)
1407	1408	1407	1397	1386-1387	v (ring sym ip, ring asym ip, $\text{CH}_2(\text{N})$ CN)
1445	1445	1446	1442	1420	v (ring asym ip, $\text{CH}_2(\text{N})$ CN)
b = bending; v = stretching; sym = symmetric; asym = asymmetric; ip = in-plane; op = out-of-plane					

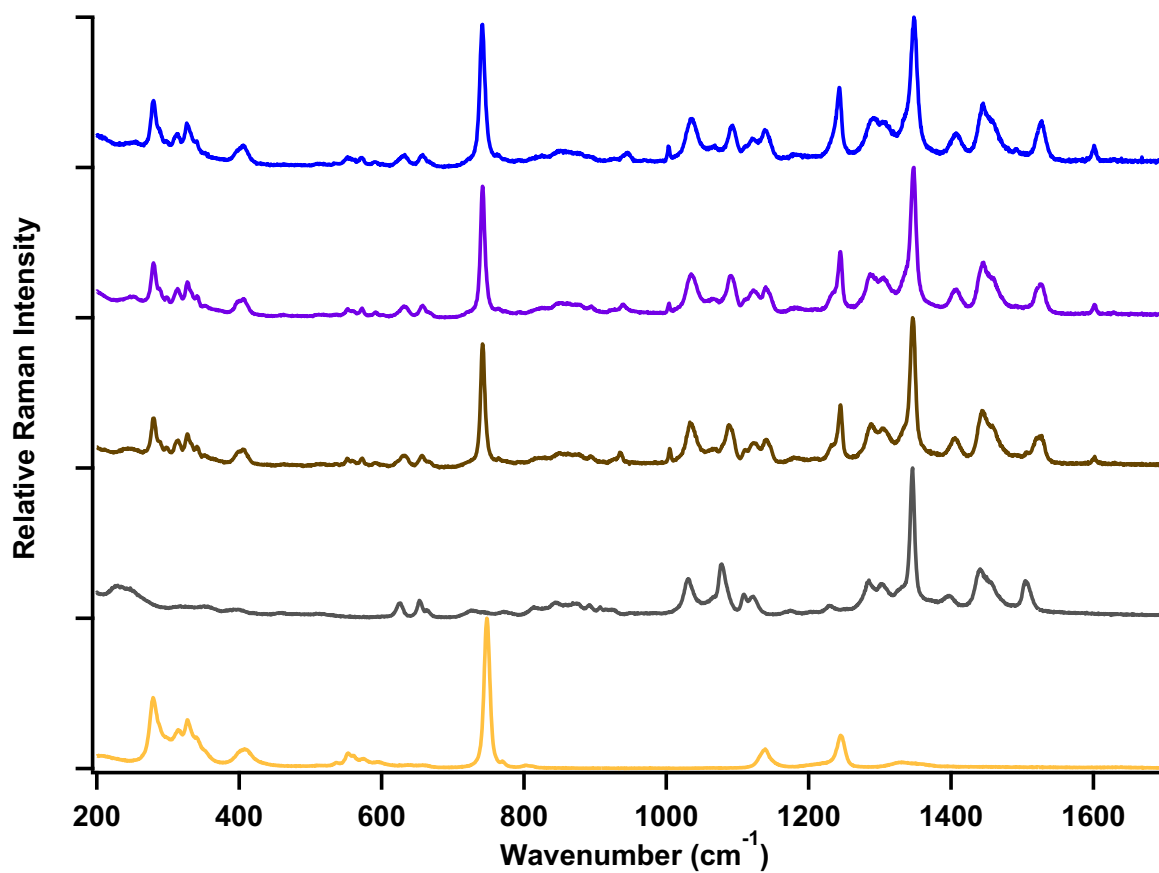


Figure S2. Normalized Raman spectra of Ni(OIm)₄(Cl)NTf₂ (blue), Co(OIm)₄(Cl)NTf₂ (purple), Mn(OIm)₄(Cl)NTf₂ (brown), 1-octylimidazole (grey) and LiNTf₂ (yellow).

Table S2. Imidazole ring vibrations, in cm^{-1} , of $\text{Ni}(\text{OIm})_4\text{NTf}_2$, $\text{Co}(\text{OIm})_4\text{NTf}_2$, $\text{Mn}(\text{OIm})_4\text{NTf}_2$ and 1-octylimidazole as measured and assignment of these vibrations from the literature.

$\text{Ni}(\text{OIm})_4(\text{Cl})\text{NTf}_2$	$\text{Co}(\text{OIm})_4(\text{Cl})\text{NTf}_2$	$\text{Mn}(\text{OIm})_4(\text{Cl})\text{NTf}_2$	1-Octylimidazole	Imidazolium-containing ILs ¹⁻³	Assignment ¹⁻³
631	632	631	625	600	b (ring op), v $\text{CH}_2(\text{N})$ CN
657	658	657	653	622-624	b (ring op), v $\text{CH}_2(\text{N})$ CN
669	668	667	665	655	b (ring op)
1036	1036	1035	1031	1022-1025	v (ring sym ip)
1348	1347	1346	1346	1339-1340	v (ring sym ip, $\text{CH}_2(\text{N})$ CN)
1407	1407	1405	1396	1386-1387	v (ring sym ip, ring asym ip, $\text{CH}_2(\text{N})$ CN)
1443	1443	1443	1439	1420	v (ring asym ip, $\text{CH}_2(\text{N})$ CN)

IR spectroscopy.

Attenuated total reflection (ATR) spectroscopy was carried out on an Alpha ATR spectrometer equipped with a diamond crystal (Bruker, Karlsruhe, D). Solid samples were pressed on the crystal with diamond surface to ensure contact.

The infrared spectra of MILs are shown in Figures S3 and S4. All spectra are quite similar. The stronger coordinating metal would be expected to produce a higher electron density in the ring system of the ligand. Therefore, the energy of the ring bonds and the frequency of the infrared bands assigned to ring vibrations serve as a means to measure the extent of the metal - imidazole interaction. The stronger metal - imidazole bond is expected to produce a higher ring frequency. The bands at about 1507, 1455, 1274 and 1227 cm^{-1} reflect the amount of electron density in the ring system.⁴ There is no significant difference in the ring stretching vibration of butylimidazole and octylimidazole counterparts for the same metal. Metal chloride vibrations are generally present in the far-infrared region and is beyond the range of our spectrometer.⁵

SO_2 symmetric and asymmetric stretches from NTf_2 anion are present in the region 1131-1140 cm^{-1} and 1345 -1360 cm^{-1} respectively. Similarly CF_3 bands are present in the region of 1165-1185 cm^{-1} .⁹

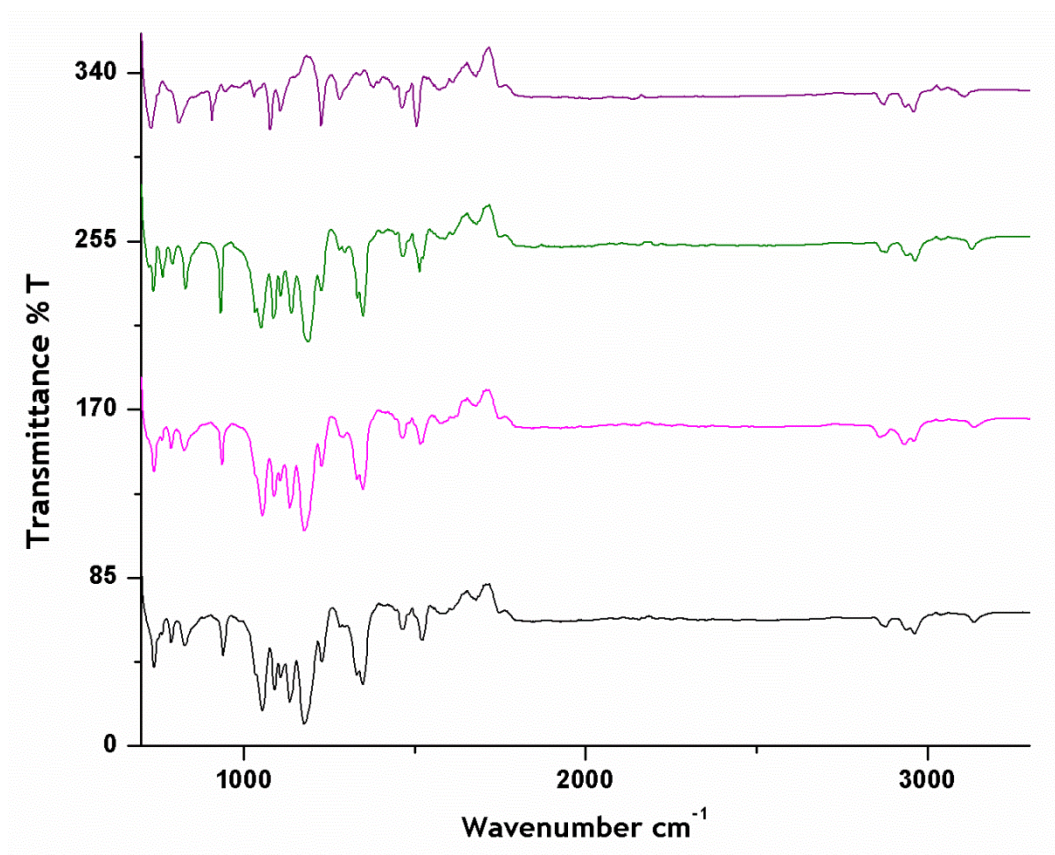


Figure S3. FTIR spectra of 1-butylimidazole (purple), Mn(BIm)₄(Cl)NTf₂ (green), Co(BIM)₄(Cl)NTf₂ (pink) and Nim(BIm)₄(Cl)NTf₂ (black)

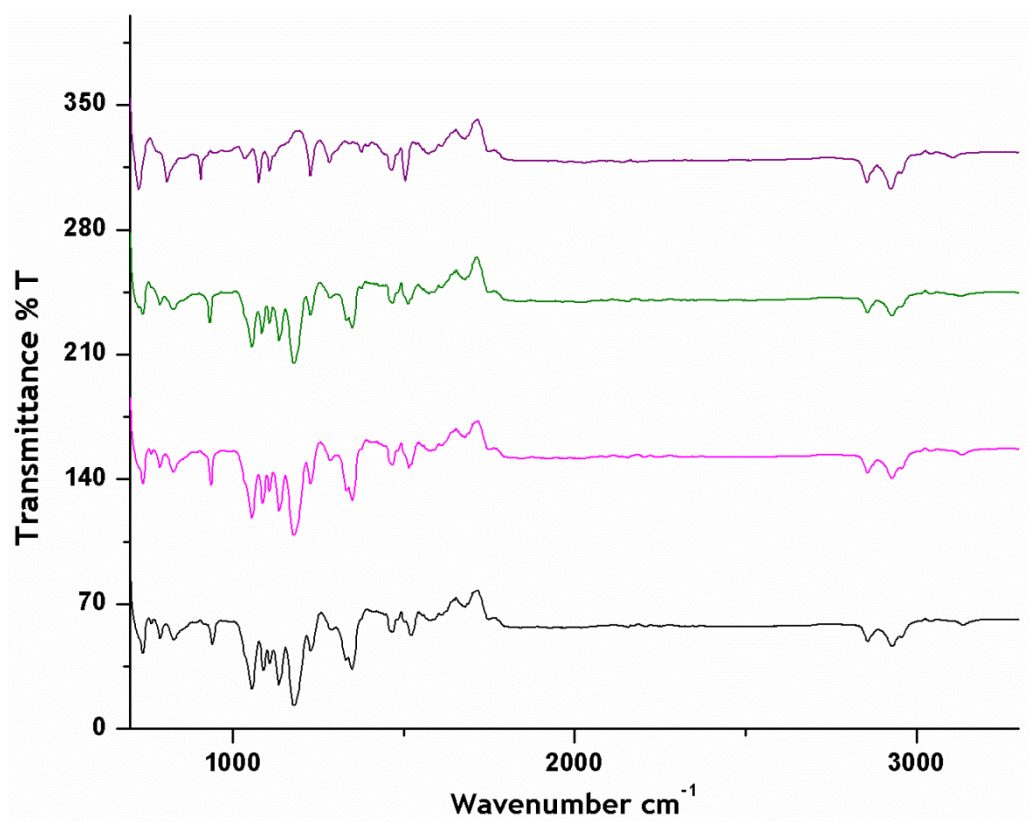


Figure S4. FTIR spectra of 1-octylimidazole (purple), $\text{Mn}(\text{OIm})_4(\text{Cl})\text{NTf}_2$ (green), $\text{Co}(\text{OIM})_4(\text{Cl})\text{NTf}_2$ (pink) and $\text{Nim}(\text{OIm})_4(\text{Cl})\text{NTf}_2$ (black)

Experimental Section

Materials:

Hydrated metal salts were dried in a vacuum oven for at least four days at 50 °C. 1-butylimidazole (98%) was purchased from Sigma Aldrich (St. Louis, MO, USA). 1-Octylimidazole (98%) was purchased from IOLITEC Inc (Tuscaloosa, AL, USA).

Elemental Analysis

Elemental analysis results (%C, %H, %N) were acquired using a PE 2100 Series II combustion analyzer (Perkin Elmer Inc., Waltham, MA).

DSC-TGA

A Netzsch STA449 F1 Jupiter (Netzsch Instruments North America, LLC; 129 Middlesex Turnpike, Burlington, MA 01803) was used to collect TGA data (thermogravimetric analysis) and DSC data (differential scanning calorimetry) in one measurement. In addition, the identity of gases evolved during the heating process was determined mass spectrometry detection with a Netzsch QMS 403 D Aeolos mass spectrometer and a Bruker Tensor 37 (Bruker Optics Inc, 19 Fortune Drive, Billerica, MA 01821). Samples weighing approximately 5 mg were heated at the heating rate of 5 °C/min in alumina crucibles with a laser drilled hole under argon as protective gas.

Ni(BIm)₄(Cl)NTf₂ (**1**)

One equivalent (millimolar) of anhydrous nickel chloride (NiCl₂) was added to four equivalents of 1-butylimidazole (BIm) in a round bottom flask. The flask was heated at 100 °C for six hours, after which the reaction mixture was dissolved in a minimum amount of methanol (≈ 10 mL) and refluxed for 24 hours at 60 °C. The solvent was removed under reduced pressure at 40 °C and the solid product was washed with diethyl ether and dried in a vacuum oven for 24 hours at 40 °C. The composition of the final product was found to be consistent with Ni(BIm)₄Cl₂ based on CHN analysis.

An aqueous solution of lithium bis[(trifluoromethyl)sulfonyl]imide (2.5 equivalents) was added drop wise to one equivalent (millimolar) of Ni(BIm)₄Cl₂ dissolved in 5 mL of water. The reaction mixture was stirred for an hour at room temperature after which the aqueous layer was discarded. The water insoluble hydrophobic component was dissolved in dichloromethane and washed several times with deionized water in a separatory funnel. The dichloromethane layer was evaporated by rotary evaporation to obtain a blue liquid in quantitative yield. The blue liquid was observed to solidify upon standing at room temperature for an extended period of time. The product was dried in a vacuum oven for 24 hours at 40 °C.

Elemental analysis (CHN): Calculated % for C₃₀H₅₄ClF₆N₉NiO₇S₂, Calculated; C, 38.95; H, 5.88; N, 13.63 Found; C, 38.97; H, 5.44; N, 13.35. IR : $\tilde{\nu}$ 3133, 2958, 2939, 2872, 1582, 1517, 1469, 1345, 1331, 1226, 1774, 1131, 1226, 1131, 1109, 1088, 1051, 941, 823, 784, 236 cm⁻¹.

Ni(OIm)₄(Cl)NTf₂ (**2**)

One equivalent (millimolar) of anhydrous nickel chloride (NiCl₂) was added to four equivalents of 1-octylimidazole (OIm) in a round bottom flask. The flask was heated at 100 °C for six hours, after which the reaction mixture was dissolved in a minimum amount of methanol (≈ 10 mL) and refluxed for 24 hours at 60 °C. Solvent was removed under reduced pressure and the solid product was washed with hexane. The composition of the product was found to be consistent with Ni(OIm)₄Cl₂ based on CHN analysis.

An aqueous solution of lithium bis[(trifluoromethyl)sulfonyl]imide (2.5 equivalents) was added dropwise to one equivalent (millimolar) of Ni(OIm)₄Cl₂ dissolved in 5 mL of acetone. Acetone was removed under reduced pressure after stirring the reaction mixture for an hour at room temperature. The hydrophobic component was extracted with dichloromethane and the dichloromethane layer was washed with water for at least four times using 5 mL aliquots. A blue liquid possessing very low viscosity was obtained after removal of the solvent. The product was obtained in a quantitative yield.

Elemental analysis (CHN): Calculated % for C₄₆H₉₂ClF₆N₉NiO₁₀S₂, Calculated; C, 45.91; H, 7.70; N, 10.47 Found; C, 45.44; H, 7.44; N, 10.86. IR : $\tilde{\nu}$ 3136, 2931, 2861, 1582, 1523, 1463, 1355, 1230, 1182, 1133, 1230, 1182, 1133, 1111, 1090, 1057, 932, 830, 781, 732 cm⁻¹.

Co(BIm)₄(Cl)NTf₂ (**3**)

One equivalent (millimolar) of anhydrous cobalt chloride (CoCl₂) was added to four equivalents of 1-butylimidazole (BIm) in a round bottom flask. The flask was heated at 100 °C for 24 hours and the reaction mixture was allowed to cool at room temperature for two hours. The solid product was washed with diethyl ether and dried in a vacuum oven for 24 hours at 40 °C. The composition of the final product was found to be consistent with Co(BIm)₄Cl₂ based on CHN analysis.

An aqueous solution of lithium bis[(trifluoromethyl)sulfonyl]imide (2.5 equivalents) was added drop wise to one equivalent (millimolar) of Co(BIm)₄Cl₂ dissolved in 5 mL of water. The reaction mixture was stirred for half an hour at room temperature after which the aqueous layer was discarded. The water insoluble hydrophobic component was dissolved in dichloromethane and was washed several times with deionized water in a separatory funnel. The dichloromethane layer was

evaporated by rotary evaporation to obtain a dark blue liquid in quantitative yield. The blue liquid was observed to solidify upon standing at room temperature for an extended period of time. The product was dried in a vacuum oven for 24 hours at 40 °C.

Elemental analysis (CHN): Calculated % for $C_{31}H_{52}ClCoF_6N_9O_4S_2$; C, 41.96; H, 5.91; N, 14.21 Found; C, 42.47; H, 5.97; N, 13.98. IR : $\tilde{\nu}$ 3136, 2963, 2866, 1582, 1517, 1468, 1349, 1328, 1279, 1230, 1176, 1138, 1106, 1090, 1052, 932, 819, 786, 732 cm^{-1} .

Mn(BIm)₄(Cl)NTf₂ (**4**)

This compound was synthesized following a procedure similar to the preparation of **1** starting from one equivalent of anhydrous manganese chloride and four equivalents of 1-butylimidazole. A yellow liquid was obtained, which gradually solidified on standing at room temperature for an extended period of time. The composition of the chloride intermediate was found to be consistent with Mn(BIm)₄Cl₂ based on CHN analysis.

Elemental analysis (CHN): Calculated % for $C_{31}H_{52}ClF_6MnN_9O_4S_2$; C, 42.15; H, 5.93; N, 14.27; Found; C, 41.85; H, 5.45; N, 14.53. IR : $\tilde{\nu}$ 3131, 2969, 2942, 2871, 1582, 1512, 1463, 1355, 1328, 1230, 1187, 1138, 1106, 1084, 1046, 1035, 938, 835, 792, 759, 732 cm^{-1} .

Co(OIm)₄(Cl)NTf₂ (**5**)

One equivalent (millimolar) of anhydrous cobalt chloride (CoCl₂) was added to four equivalents of 1-octylimidazole (OIm) in a round bottom flask. The flask was heated at 100 °C for 24 hours after which the reaction mixture was allowed to cool at room temperature for two hours to obtain a dark blue solid. The solid product was washed with hexane and dried in a vacuum oven for 24 hours at 40 °C. The composition of the final product was found to be consistent with Co(OIm)₄Cl₂ based on CHN analysis.

One equivalent (millimolar) of Co(OIm)₄Cl₂ was dissolved in acetone (5 mL) and 2.5 equivalents of an aqueous solution of lithium bis(trifluoromethanesulfonyl)imide was added drop wise to it. Acetone was removed under reduced pressure after stirring the reaction mixture for an hour at room temperature. The hydrophobic component was extracted with dichloromethane and the dichloromethane layer was washed with water for at least four times using 5 mL aliquots. A pink

liquid possessing very low viscosity was obtained after removal of the solvent. The product was obtained in quantitative yield.

Elemental analysis (CHN): Calculated % for $C_{46}H_{80}ClCoF_6N_9O_4S_{22}$; C, 50.42; H, 7.36; N, 11.51 Found; 50.04, 7.30, 11.92. IR : $\tilde{\nu}$ 3136, 2969, 2936, 2861, 1572, 1507, 1463, 1349, 1339, 1279, 1236, 1187, 1138, 1106, 1084, 1057, 932, 830, 792, 738 cm^{-1} .

$Mn(OIm)_4(Cl)NTf_2$ (**6**)

This compound was prepared following a procedure similar to the synthesis of **5** starting from one equivalent of anhydrous manganese chloride and four equivalents of 1-octylimidazole. A very low viscous yellow liquid was obtained in a quantitative yield.

Elemental analysis (CHN): Calculated % for $C_{46}H_{80}ClF_6MnN_9O_4S_{22}$; C, 50.61; H, 7.39; N, 11.55 Found; C, 50.91; H, 7.84; N, 11.15. IR : $\tilde{\nu}$ 3131, 2931, 2866, 1577, 1517, 1474, 1355, 1333, 1236, 1187, 1228, 1100, 1079, 1052, 932, 830, 776, 738 cm^{-1} .

Thermal Properties

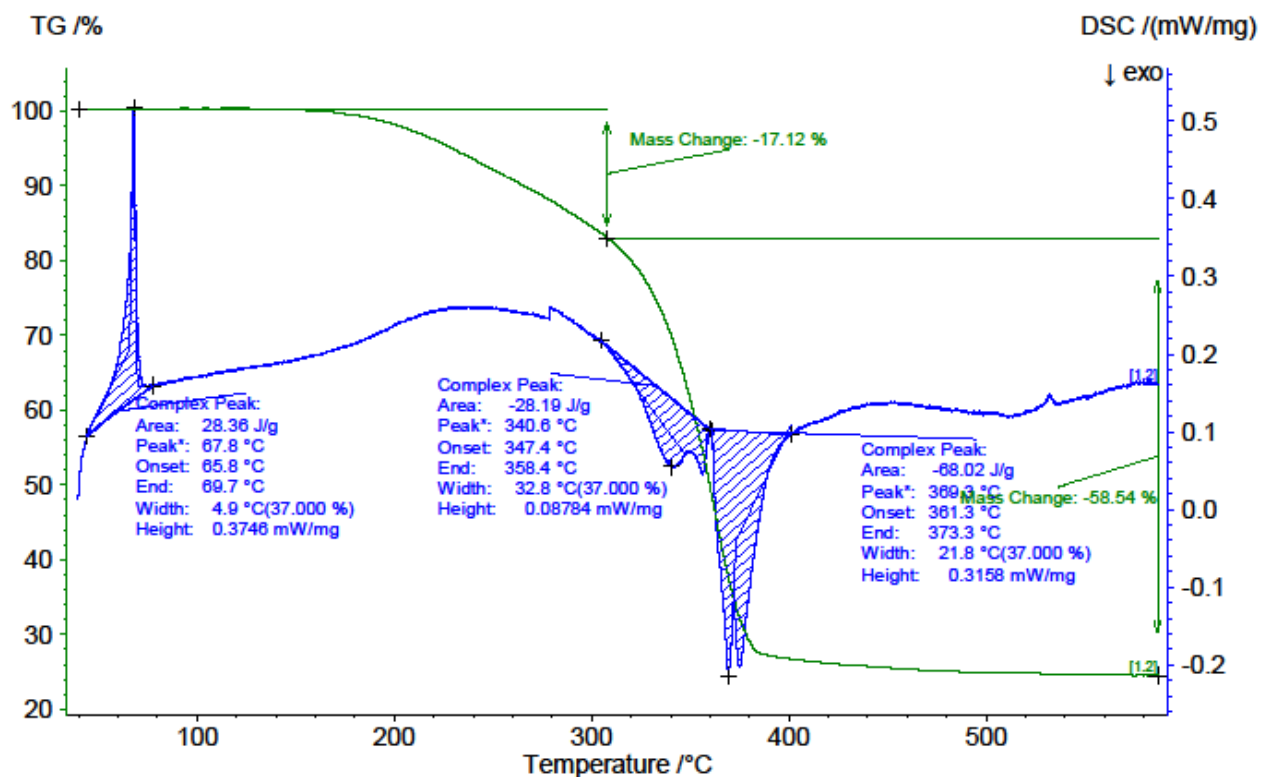


Figure S5. TG and DSC thermograms of the compound Ni(BIm)₄(Cl)NTf₂ (2).

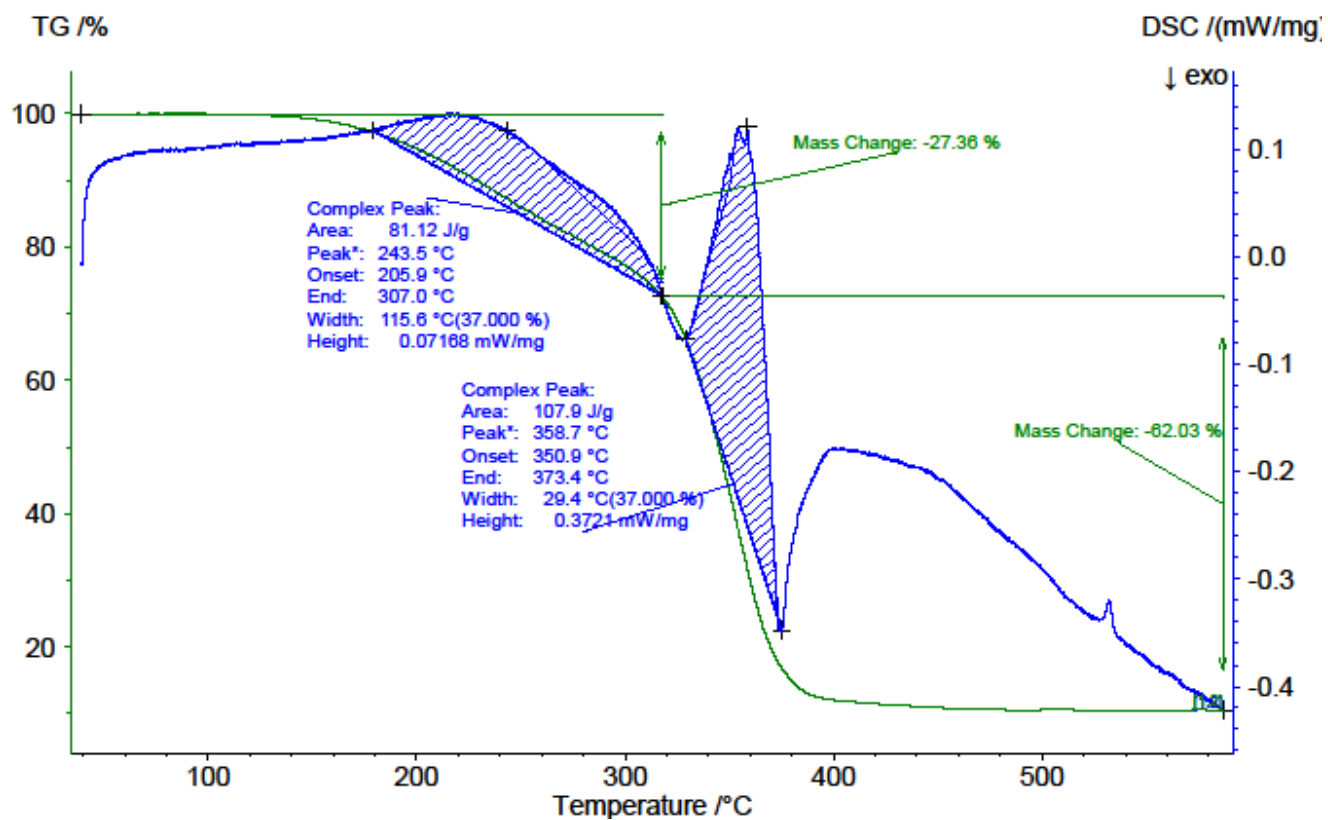


Figure S6. TG and DSC thermograms of the compound $\text{Ni}(\text{OIm})_4(\text{Cl})\text{NTf}_2$ (**2**).

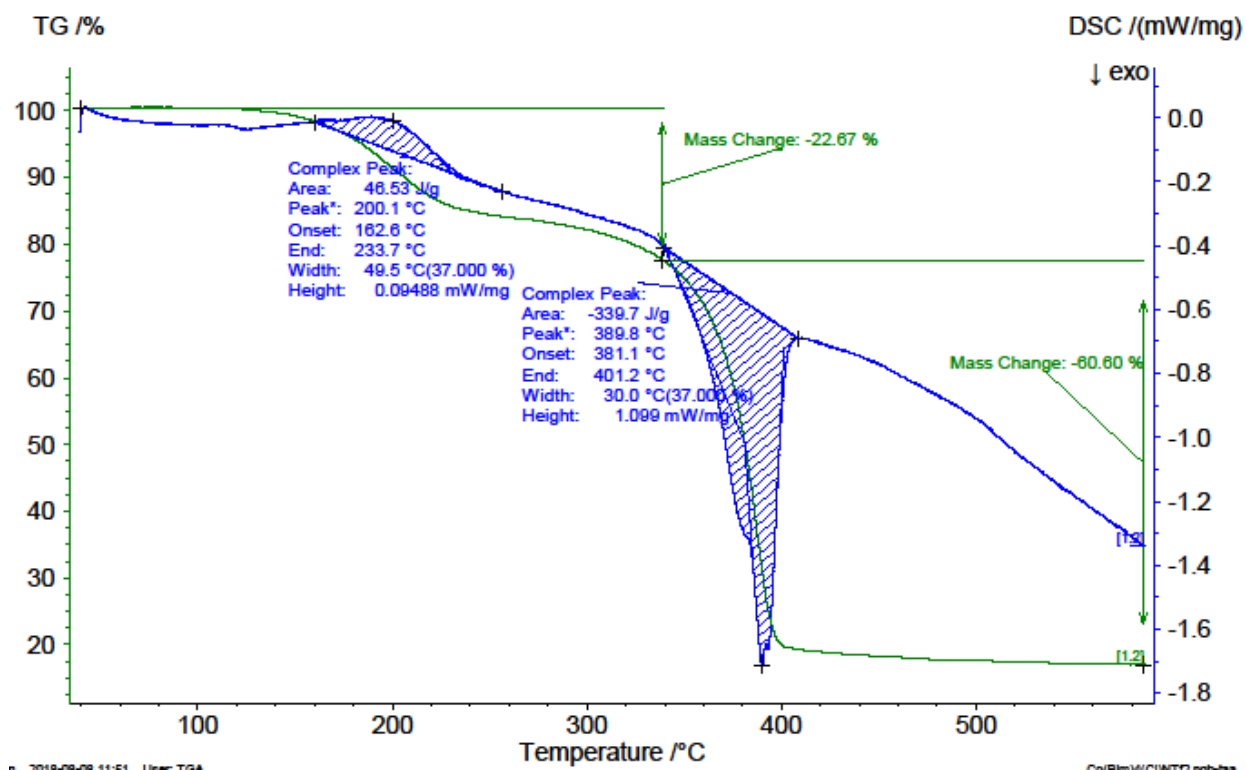


Figure S7. TG and DSC thermograms of the compound $\text{Co}(\text{BIm})_4(\text{Cl})\text{NTf}_2$ (**3**).

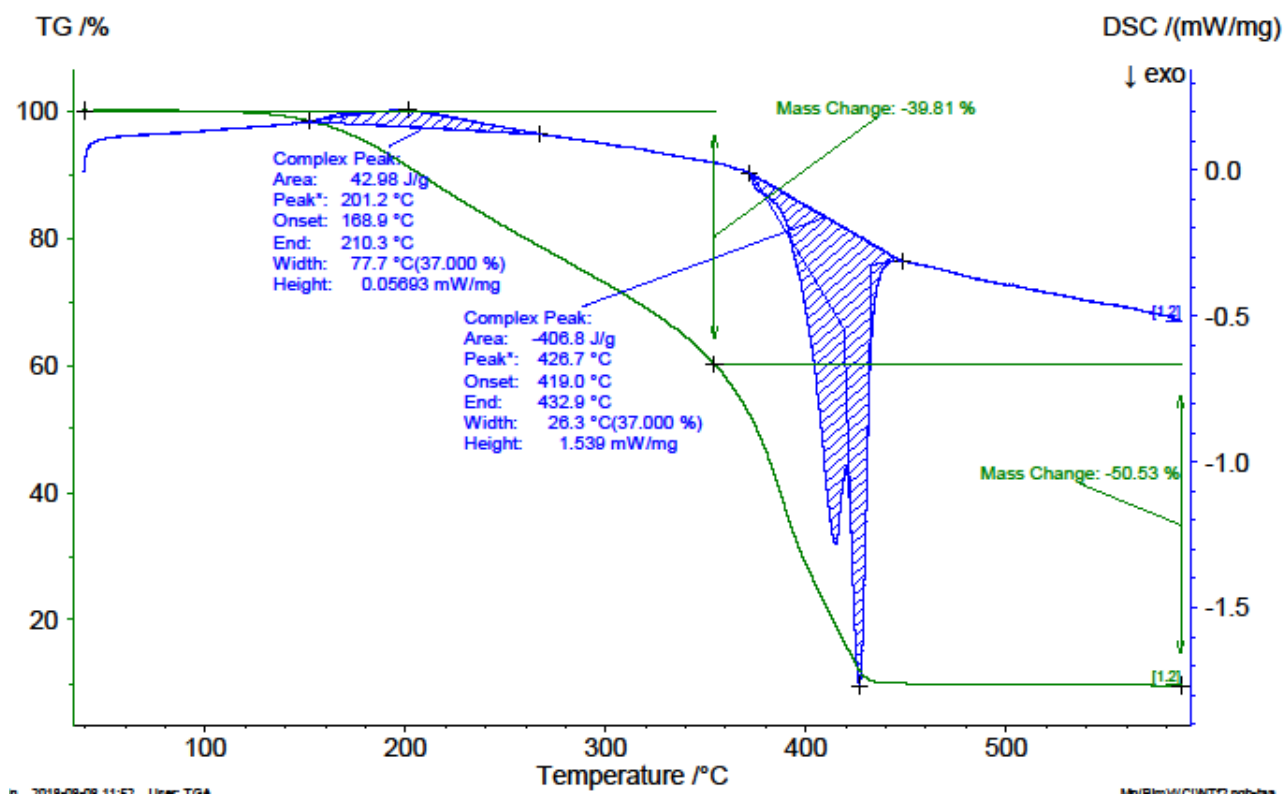


Figure S8. TG and DSC thermograms of the compound $\text{Mn}(\text{BIm})_4(\text{Cl})\text{NTf}_2$ (**4**).

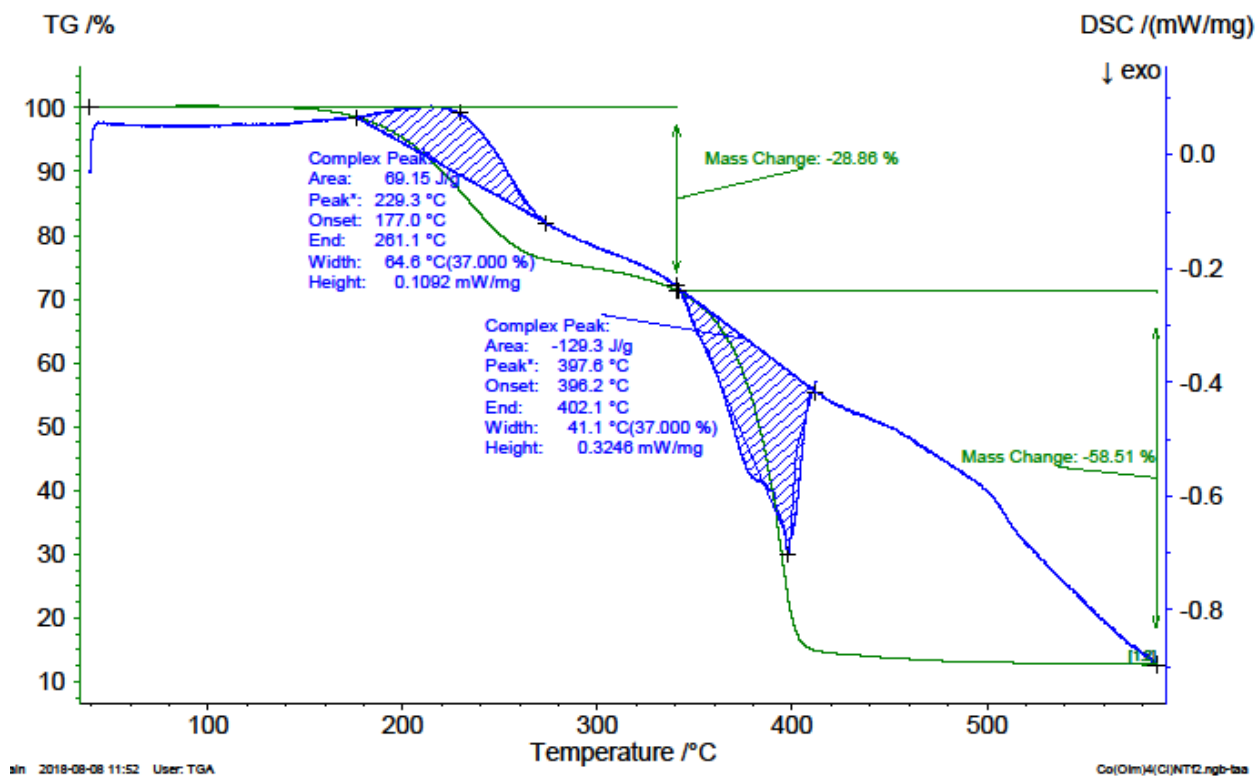


Figure S9. TG and DSC thermograms of the compound Co(OIm)₄(Cl)NTf₂ (**5**).

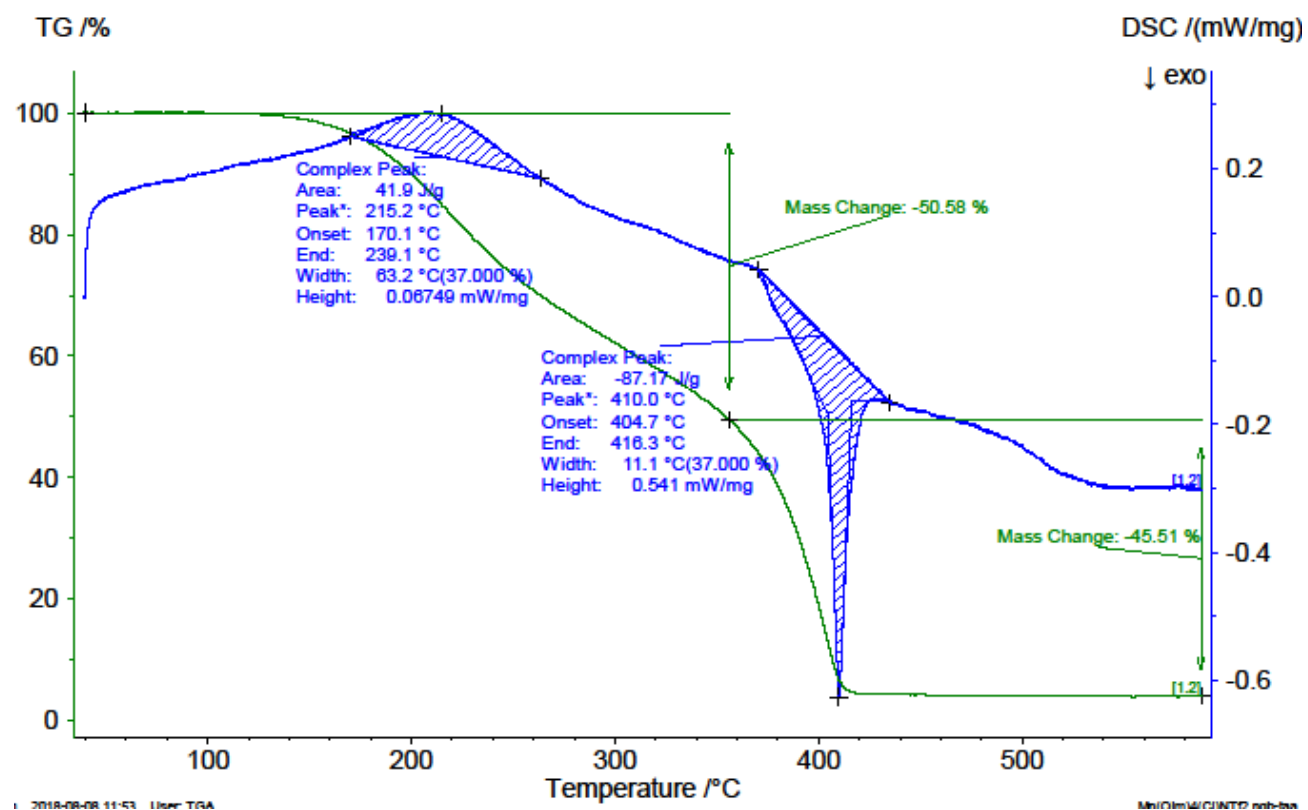


Figure S10. TG and DSC thermograms of the compound $\text{Mn}(\text{OIm})_4(\text{Cl})\text{NTf}_2$ (6).

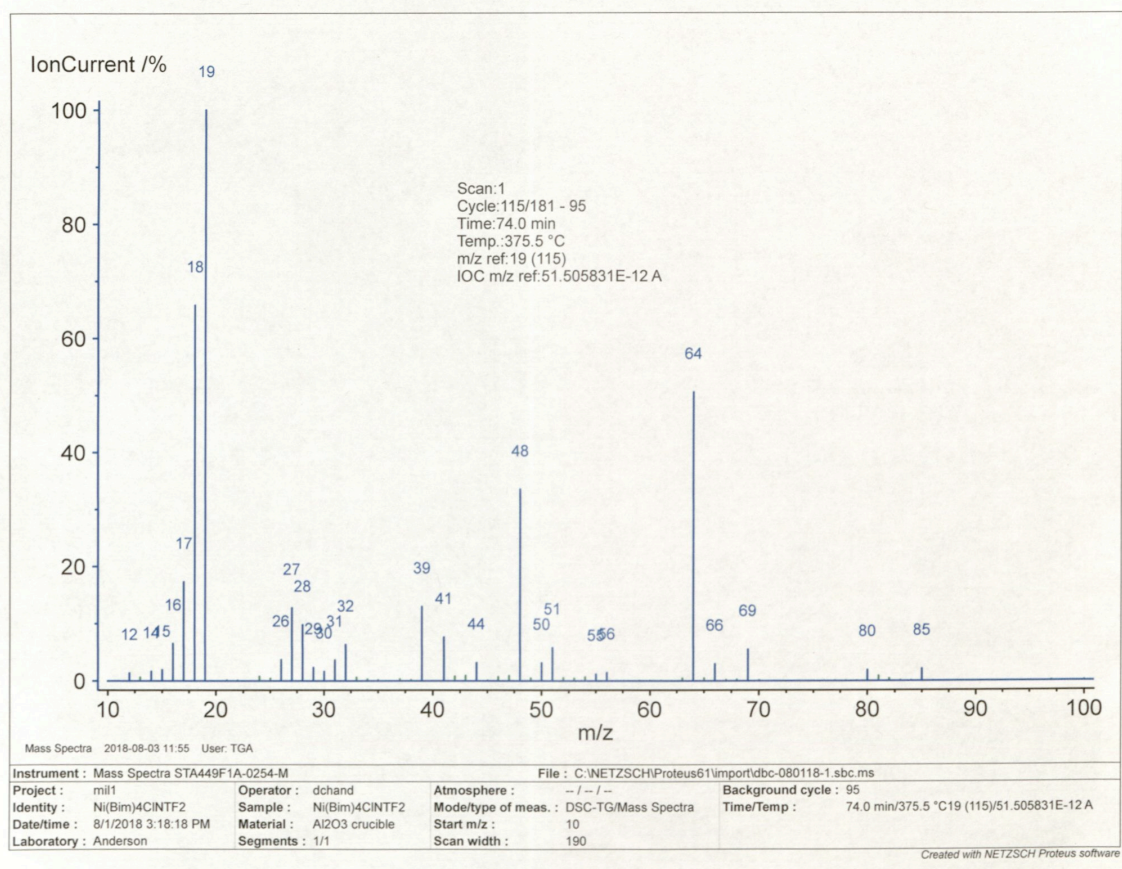


Figure S11. Mass spectrum of the evolved gases during the TGA experiment for the Ni(BIm)₄(Cl)NTf₂ MIL.

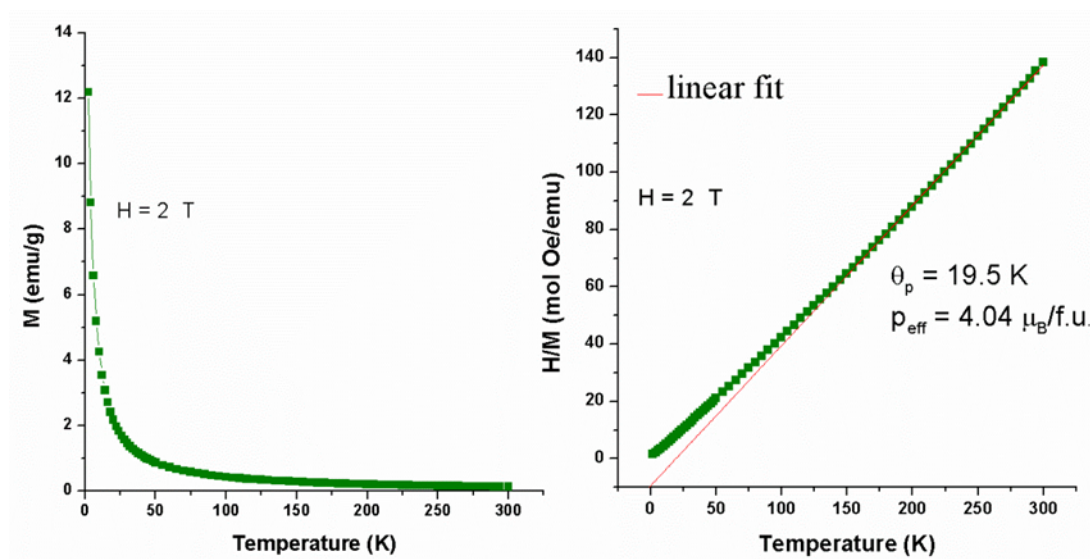


Figure S12. Magnetization of the $\text{Mn}(\text{OIm})_4(\text{Cl})\text{NTf}_2$ MIL measured as a function of temperature (20000 Oe applied magnetic field) is shown in the left and Curie-Weiss fit of the linear portion of the reciprocal susceptibility at the right.

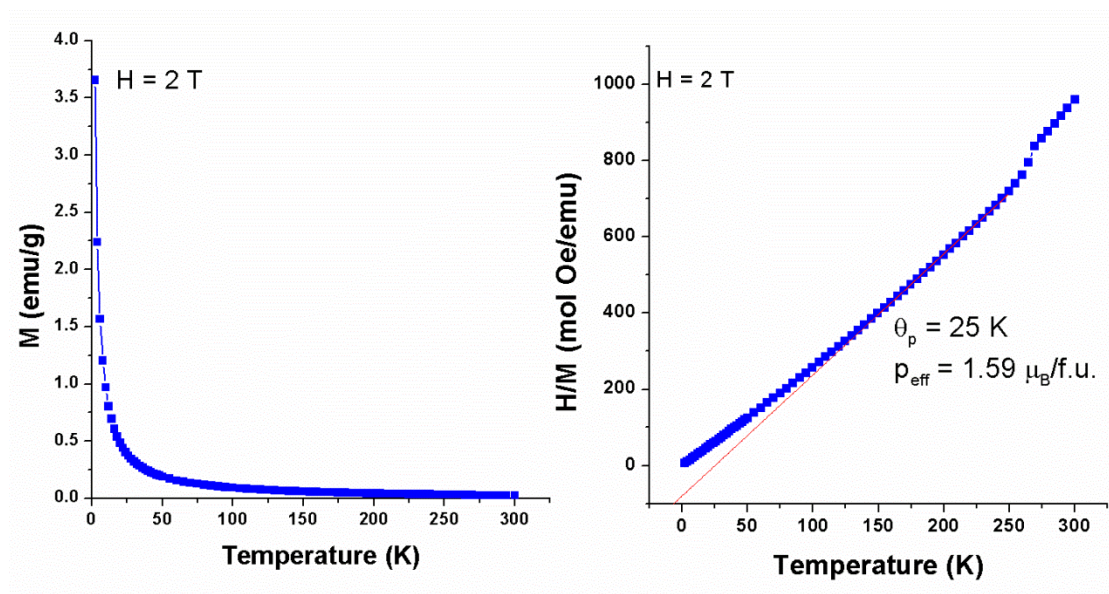


Figure S13. Magnetization of the $\text{Ni}(\text{BIm})_4(\text{Cl})\text{NTf}_2$ measured as a function of temperature in a 20000 Oe applied magnetic field (left) and Curie-Weiss fit of the linear portion of the reciprocal susceptibility (right).

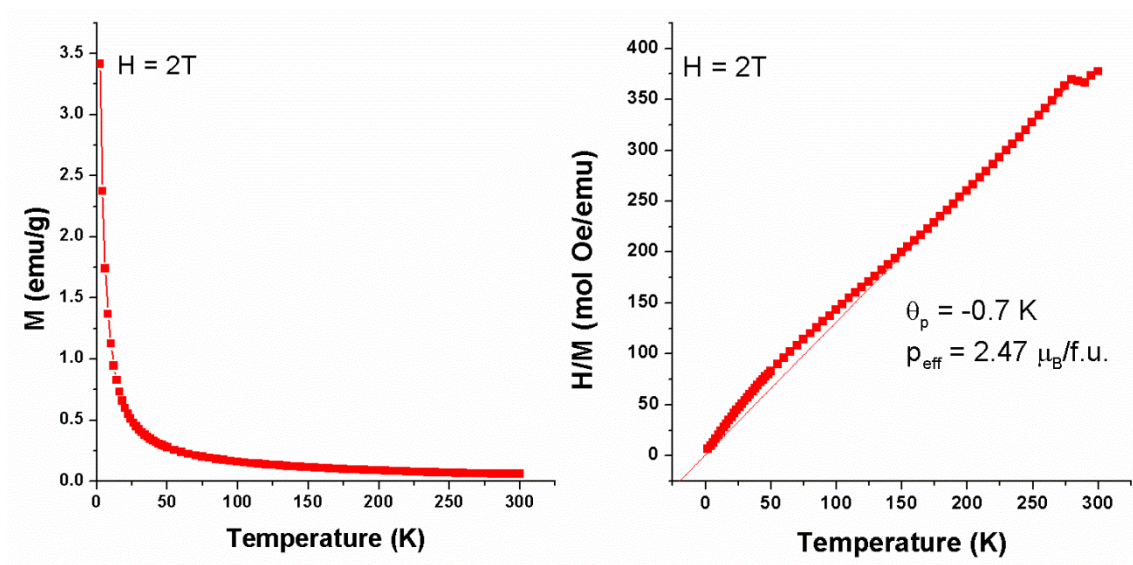


Figure S14. Magnetization of the $\text{Co}(\text{BIm})_4(\text{Cl})\text{NTf}_2$ measured as a function of temperature in a 20000 Oe applied magnetic field (left) and Curie-Weiss fit of the linear portion of the reciprocal susceptibility (right).

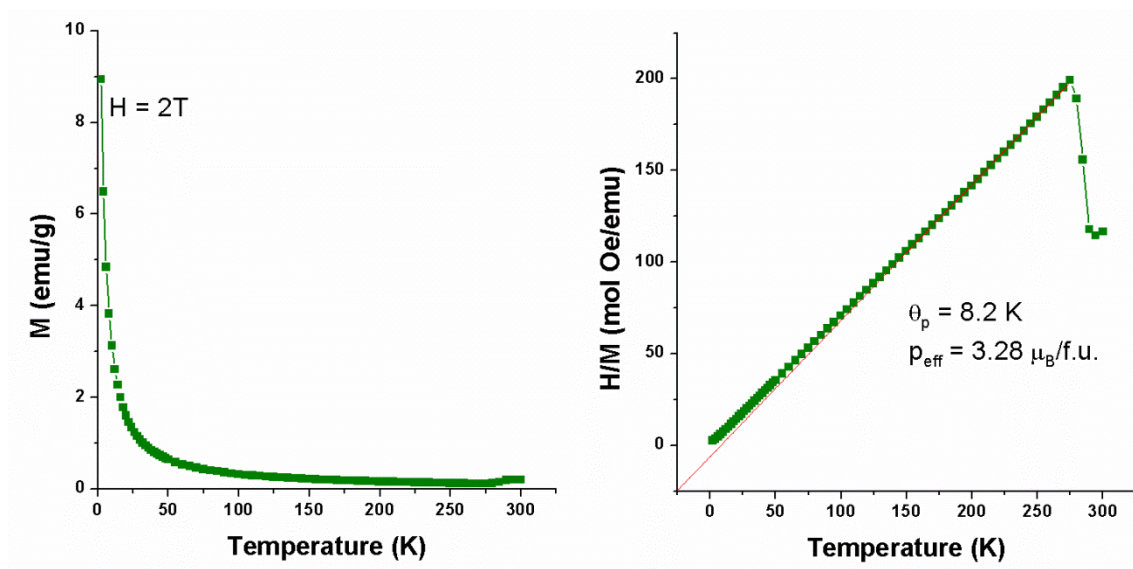


Figure S15. Magnetization of the $\text{Mn}(\text{BIm})_4(\text{Cl})\text{NTf}_2$ measured as a function of temperature in a 20000 Oe applied magnetic field (left) and Curie-Weiss fit of the linear portion of the reciprocal susceptibility (right).

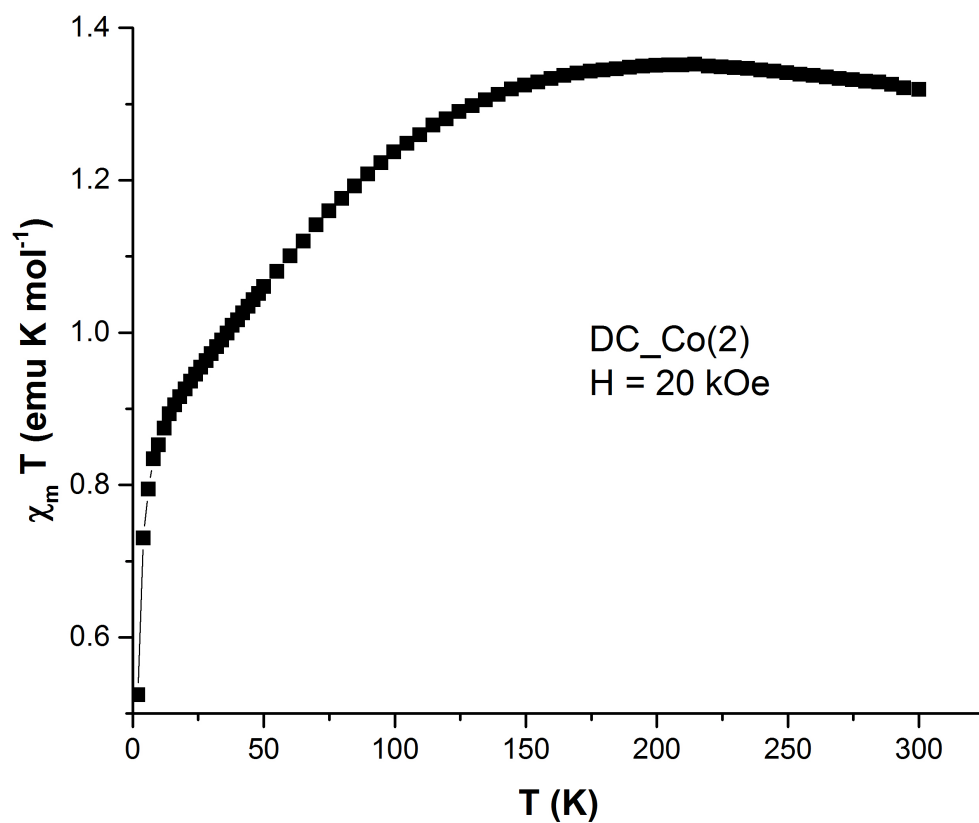


Figure S16. Product of magnetic susceptibility and temperature (χT) as a function of temperature for the $\text{Co}(\text{OIm})_4(\text{Cl})\text{NTf}_2$ MIL, measured at $H = 20000$ Oe.

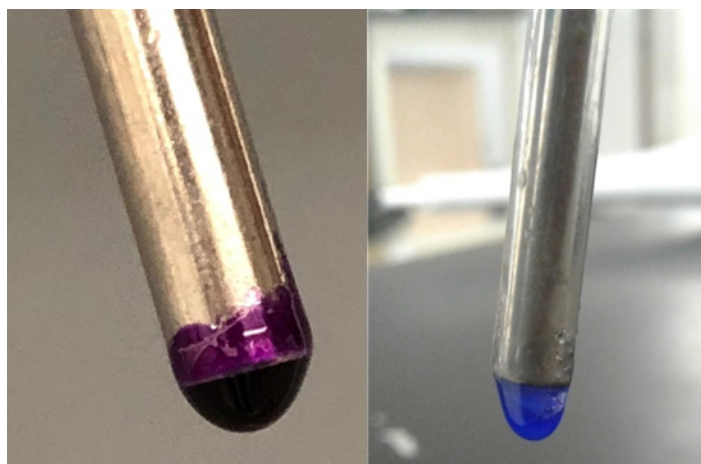


Figure S17. Manipulation of MILs by a Neodymium magnet (0.66 T), $\text{Co}(\text{BIm})_4(\text{Cl})\text{NTf}_2$ (left) and $\text{Ni}(\text{BIm})_4(\text{Cl})\text{NTf}_2$ (right)

References

1. Heimer, N. E.; Del Sesto, R. E.; Meng, Z.; Wilkes, J. S.; Carper, W. R. *J. Mol. Liq.*, 2006, **124**, 84-95.
2. Holomb, R.; Martinelli, A.; Albinsson, I.; Lassegues, J. C.; Johansson, C. P.; Jacobsson, P. *J. Raman Spectrosc.*, 2008, **39**, 793-805.
3. Talaty, E. R.; Raja, S.; Storhaug, V. J.; Dölle, A.; Carper, W. R. *J. Phys. Chem. B*, 2004, **108**, 13177-13184
4. Clark, R. J. H.; Williams C. S. *Inorg. Chem.* 1965, **4**, 350–357.
5. Hanke, K.; Matin, M.; Schwaab, G.; Havenith, M.; Wolke, C. T.; Gorlova, O.; Johnson, M. A.; Kar, B. P.; Sander, W.; Sanchez-Garcia, E. *Phys. Chem. Chem. Phys.*, **2015**, 17, 8518—8529.